

Accelerate High-Quality Diffusion Models with Inner Loop Feedback

Matthew Gwilliam^{1*}† Han Cai² Di Wu² Abhinav Shrivastava¹ Zhiyu Cheng^{2*}

¹University of Maryland, College Park ²NVIDIA



Figure 1. PixArt-sigma 1024x1024 images, generated with 20 steps using DPM-Solver++ (top) vs. PixArt-sigma with caching (middle) vs. PixArt-sigma with **ILF** (bottom). ILF produces high quality images **1.8x** faster, measured on H100 GPUs.

Abstract

We propose **Inner Loop Feedback (ILF)**, a novel approach to accelerate diffusion models’ inference. ILF trains a lightweight module to predict future features in the denoising process by leveraging the outputs from a chosen diffusion backbone block at a given time step. This approach exploits two key intuitions; (1) the outputs of a given block at adjacent time steps are similar, and (2) performing partial computations for a step imposes a lower burden on the model than skipping the step entirely. Our method is highly flexible, since we find that the feedback module itself can simply be a block from the diffusion backbone, with all settings copied. Its influence on the diffusion forward can be tempered with a learnable scaling factor from zero initial-

ization. We train this module using distillation losses; however, unlike some prior work where a full diffusion backbone serves as the student, our model freezes the backbone, training only the feedback module. While many efforts to optimize diffusion models focus on achieving acceptable image quality in extremely few steps (1-4 steps), our emphasis is on matching best case results (typically achieved in 20 steps) while significantly reducing runtime. ILF achieves this balance effectively, demonstrating strong performance for both class-to-image generation with diffusion transformer (DiT) and text-to-image generation with DiT-based PixArt-alpha and PixArt-sigma. The quality of ILF’s 1.7x-1.8x speedups are confirmed by FID, CLIP score, CLIP Image Quality Assessment, ImageReward, and qualitative comparisons. Project information is available at [this website](#).

*Correspondence to: Matthew Gwilliam (mgwillia@umd.edu), Zhiyu Cheng (zhiyuc@nvidia.com).

†Work completed during internship at NVIDIA.

1. Introduction

Since its introduction as an alternative to generative adversarial networks (GANs) [9] for image synthesis [7], diffusion has been one of the most prominent methods for generative tasks. These methods deliver stable training, high quality generations, and easy alignment to a variety of conditions for generative tasks [51]. However, the actual generation process is quite expensive. While GANs generate images in a single model forward pass, diffusion models require many model forward passes to iteratively progress from random noise to clean images. As a result, many researchers have focused on trying to improve the efficiency of diffusion models, while retaining the quality. Some of these are training-free, focusing on caching features for cheaper inference; others involve expensive distillation to dedicated-purpose few step models.

We propose inner loop feedback (ILF) for diffusion models, seeking to achieve higher quality at better efficiency than caching, as shown in Figure 1, without the training cost and inflexibility of distillation-based approaches. With this approach, we can take any frozen pre-trained transformer-based diffusion model, and make each of its steps more powerful by training a new block, the feedback module, to take features from a block b at one step, t , and predict features for prior blocks $b - 1, b - 2, \dots, b - l$ corresponding to the next step, $t - r$, as shown in Figure 2. In contrast to these distillation-based methods that seek to learn models that can achieve *reasonable* quality with 4 or fewer inference steps, we focus instead on matching or surpassing the *best-case* performance of the original model, in less time. Furthermore, with our approach, one does not need to store an entire additional set of models weights, instead only those corresponding to the lightweight learnable module.

Caching literature reveals that features for U-Net diffusion models are very similar for a given block, b , at adjacent time steps, t and $t - r$ [26, 48]. We find this remains consistent for transformer-based diffusion models, in Figure 3, with an implementation described in Section 2.2. Caching methods leverage this concept to skip computation for certain blocks at certain steps, simply re-using the prior features. However, as Figure 3 also shows, leveraging these similar adjacent features changes the make-up of the features themselves.

The caching schedule itself is noticeable; since features are cached on every other step, instead of smooth change over blocks and time, feature pairs become noticeable on the time axis. Furthermore, except for the last steps, the final model outputs become less distinct between neighboring steps. The same phenomenon manifests when we consider how the features evolve across blocks (Figure 4); once we introduce caching, features of the last block do not become as dissimilar to the first step for the steps on which the

caching occurs. This is clearly not optimal, and results in poorer quality images, as shown in Figure 5. Caching often loses key details, and produces blurrier, less appealing generations. This motivates our inner loop feedback; we want to take advantage of the similarity between blocks across time, like caching, but without compromising the quality of the final images.

For flexibility of adaptation to novel architectures, we propose leveraging the model architecture itself to design the feedback module. The module consists of a single block, copied from the block design of the corresponding pre-trained diffusion transformer backbone. That is, for the basic DiT, our feedback module is a single DiT block. This way, our feedback handles conditions, input sizes, and output sizes in the same way as the base model.

Different diffusion models have learned weight values of varying magnitudes, and training quickly, without overfitting or diverging, is quite challenging. To allow for fast training we use distillation. However, unlike prior works, we do not have a separate teacher and student. Instead, the model without feedback is the teacher, and the model with feedback is the student – but only the feedback is learnable. Furthermore, while prior works perform multiple teacher iterations, which is expensive, we propose an approach that allows us to only use one. We find this Fast Approximate Distillation works equally well, at lower cost. To avoid overfitting, we add Learnable Feedback Rescaling, where we learn an integer scaling term on the feedback before we add it to the features in the pretrained model. Initializing this to zero allows the model to learn quickly from the distillation, without diverging due to excessively large error. Neither Fast Approximate Distillation nor Learnable Feedback Rescaling require any hand-tuned hyperparameters, allowing for easy implementation and extension to other models and data.

One challenge introduced by our approach is that since we attempt to predict features corresponding to future steps, it is not immediately clear how to set the noise steps for the backbone and scheduler. While we find that using default schedulers works well, this does not hold true for the model backbone itself, where we must use a rescaled step for the time conditioning at inference time. Furthermore, we find that for larger inner loops, it is often best to skip feedback on some steps altogether. We instantiate these findings collectively as Feedback-aware Inference Scheduling.

In summary, we achieve high quality efficient generation with the following contributions:

- We propose diffusion with Inner Loop Feedback (ILF), a feedback mechanism which creates a powerful inner loop within transformer-based diffusion backbones for optimal time-quality trade-offs.
- We develop Learnable Feedback Rescaling and Fast Approximate Distillation for speedy training, and Feedback-

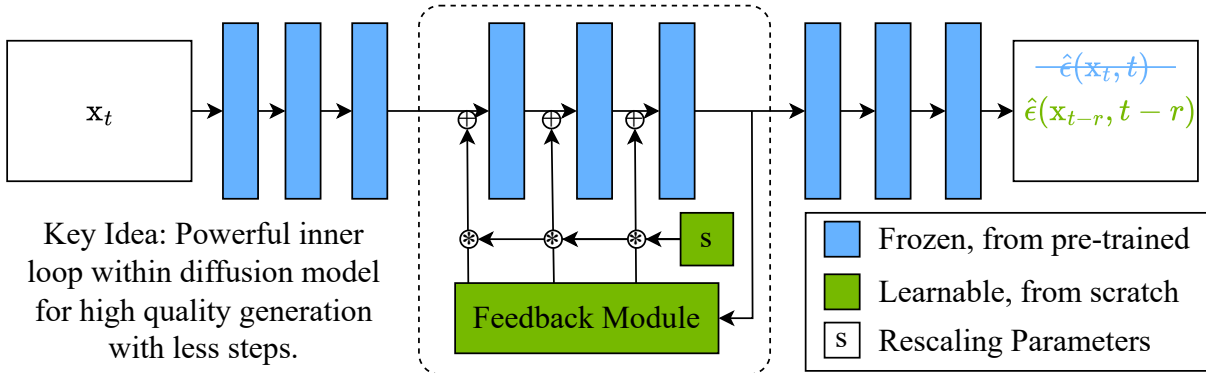


Figure 2. ILF uses a lightweight, learnable feedback module to create a powerful inner loop within a diffusion model. Instead of computing a forward through all backbone blocks, in order, we choose some block, provide its output features as input to the feedback module, then *feed* those features *back* to some earlier blocks in the model, modified by a learnable scaling term. The feedback’s objective is essentially to predict features corresponding to some future diffusion time step, so the resulting noise prediction is more reliable for the model’s current step.

aware Inference Scheduling to adaptively leverage the power and speed of ILF at inference time.

- We achieve superior results to caching for 1.7x-1.8 speedups compared with the baseline model, with an average +7.9 improvement for Image Reward, +0.14 CLIP, -0.22 MJHQ FID, and +1.4 CLIP IQA Score.

2. Related Work

2.1. Diffusion for Image Generation

Diffusion Fundamentals. Diffusion models [7, 12, 30] consider a forward noising process. Given some distribution $q(x_0)$, a sample x_0 is noised in steps accordingly to a schedule, $\{\beta_t\}_{t=1}^T$, where at any time step t , we can calculate the noised sample, x_t , as

$$x_t = \sqrt{\bar{\alpha}_t}x_0 + \sqrt{1 - \bar{\alpha}_t}\epsilon, \epsilon \sim \mathcal{N}(0, \mathbf{I}) \quad (1)$$

with $\alpha_t := 1 - \beta_t$ and $\bar{\alpha}_t := \prod_{i=0}^t \alpha_i$. The diffusion model is instantiated as a neural network that reverses the forward noising process, by predicting ϵ_t that ought to be removed from x_t to predict x_{t-1} .

Model Architecture. Early diffusion models rely on U-Net architectures [7, 12, 38], processing images (or noised images) into features in an encoder, then back to images (or noise, in pixel space) with a decoder, with connections between symmetric encoder and decoder blocks. For the sake of efficiency, subsequent methods perform diffusion on latent representations [37] from pre-trained variational auto-encoders [17]. Originally proposed for image generation, these models are also well-suited for image editing [3, 16] and video generation [2, 13, 23]. These models can be conditioned on text encodings [29, 33, 36, 39, 42] from power-

ful models including CLIP [34] and T5 [35]. Recently, to allow for more flexible scaling, transformer-based diffusion models [1, 32] have become the predominant architecture for state-of-the-art diffusion models [4–6, 8, 23]. Due to the recent trend towards diffusion transformers, we choose to focus our work primarily on this family of architectures, including the original DiT [32] for class-to-image generation, and PixArt-alpha [4] and PixArt-sigma [5] for text-to-image generation.

Inference Scheduling. While diffusion models are typically trained on 1000-step schedules, inference is performed at much lower steps, with schedulers to handle timestep spacing, as well as forward and reverse noising [15, 24, 46]. Recent work investigates non-uniform, model-specific timestep spacing [41]. We propose substantial inference-time improvements for ILF in Section 3.3, but these are all compatible with existing inference schedulers.

2.2. Faster Diffusion Inference

A significant body of work focuses on speeding up diffusion inference to generate good images in fewer steps. The majority of these approaches can be divided between training-free caching approaches, and training-based distillation approaches.

Caching. Prior caching work focuses mainly on U-Net architectures. While the methods share a key intuition, that features are similar at adjacent time steps, their configurations differ. Some cache only encoder features [21], others cache outer layers of both encoder and decoder [26], and others automatically discover ways to cache a variety of layers [48]. Concurrent work has started to approach caching for DiTs [22, 45], including some work which focuses on learnable routing for the caching [27]. One major differ-

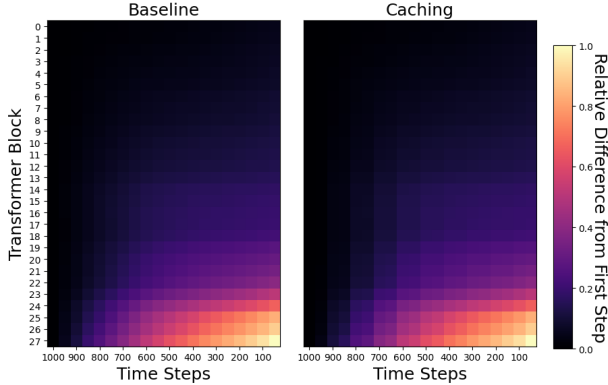


Figure 3. Change in features across time steps, measured for each block as difference from that block’s feature at $t = 1000$, normalized by dividing by the maximum difference across both plots. Caching reduces the degree to which the features change over time.

ence between U-Nets and DiTs is the absence of encoder-decoder distinction, which changes the caching approach substantially. Furthermore, many of these approaches focus on generation of lower resolution images, using class conditioning, with many time steps. By contrast, more modern text-to-image models use fewer steps. With fewer steps, the feature maps change much less smoothly over time, mitigating the suitability of caching; furthermore, errors and blurriness become even more glaring at higher resolution (see Figure 5 for examples). Nevertheless, we implement caching as a point of comparison for ILF.

For this caching, we store the attention and feedforward results for each cacheable block on the first step. Then, at subsequent steps, for all cacheable blocks, we only recompute attentions and feedforwards on every other step; otherwise, we simply add the stored results to the new input hidden states. We illustrate this approach in Figure 6, and compare it to ILF. Unlike caching approaches, we train ILF with lightweight external module that increases the complexity of each forward pass, which allows us to achieve much better quality-speed trade-offs at inference time.

Training or Finetuning. Some approaches learn lightweight modules for predicting skip connections [14] or predicting steps based on prompt complexity [53]. The majority of the literature tends to focus on knowledge distillation [11], progressive distillation [43], guidance distillation [28], and consistency distillation [25]. Unlike the majority of these works, we do not focus on generating images of *acceptable* quality in extremely low steps [18, 19, 44, 50, 52]; instead, we seek to synthesize *maximum* quality images in the fewest possible steps. We also do not distill an entire network, instead learning only a small external module. Due to these two factors, we do not perform direct numeri-

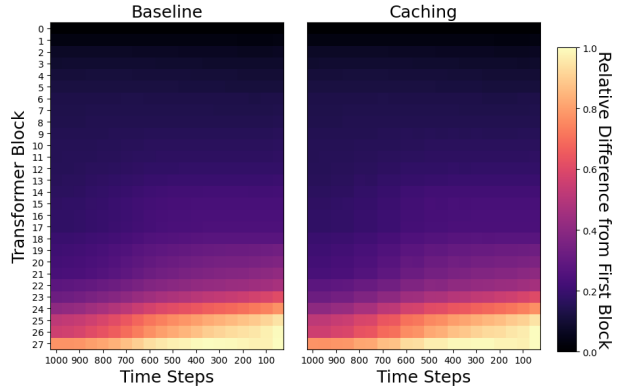


Figure 4. Change in features across blocks, measured for each block at each time step as difference from the first block’s feature at that time step, normalized as in Figure 3. The trend with caching is similar here as when measuring difference over time.

cal comparisons with these methods.

3. Approach

3.1. Inner Loop Feedback Design

We propose a lightweight learnable module that leverages similar intuitions to caching, but with a different mechanism and superior results. This method, illustrated in Figure 2, starts with some pre-trained, transformer-based diffusion model. Standard diffusion forward passes attempt to predict $\hat{\epsilon}(x_t, t)$, for some noised latent x_t and time step t . By contrast, with our feedback mechanism, we attempt to make the forward pass more powerful, where we instead predict $\hat{\epsilon}(x_{t-r}, t-r)$, where r is some positive integer, meaning $t-r$ is some subsequent time step. This allows us to generate high quality images with fewer, but more powerful, inference steps.

We design the feedback module itself by simply copying the architecture of the model blocks themselves, such that for a standard N block DiT, we introduce a $(N+1)$ th block. However, instead of simply appending, prepending, or inserting the block, we dramatically alter the flow of information. We first set a location for the inner loop, denoted by the beginning (b) block, B_b , and the ending (e) block B_e . For some time step t , the feedback module takes the following as input: $f_{e,t}$ (which is the output of B_e at time step t), the embedded time condition, and the embedded text conditions. The feedback model gives its output, f_{feed} . We then rescale the f_{feed} for separately for each block in the inner loop, $\{B_b, B_{b+1}, \dots, B_e\}$, by multiplying each by its corresponding learnable floating point scaling factor, $\{s_b, s_{b+1}, \dots, s_e\}$. For the first block, B_b , we compute its



Figure 5. We compare typical 20 step diffusion inference to caching for PixArt-alpha, 512x512 images. We cache the middle 14 blocks, recomputing features every other step. Caching, while more efficient, sometimes results in quality degradation – loss of detail (no faces in leftmost image), less appealing design (middle images), and blurriness (rightmost image, zoom in on eyes, ears, hair, and mouth).

result as

$$f_{b,t-r} = f_{\text{feed}} * s_b + f_{b-1,t} \quad (2)$$

We compute the features outputs of any subsequent block, $f_{i,t-r}$ for block B_i , with

$$f_{i,t-r} = f_{\text{feed}} * s_i + f_{i-1,t-r} \quad (3)$$

3.2. Training Inner Loop Feedback

One cannot train this feedback mechanism with basic random initialization; the magnitude of the feedback will be too large, and the training will diverge. Furthermore, standard training is needlessly slow. To keep the training stable and time-efficient, we leverage both novel Learnable Feedback Rescaling as well as Fast Approximate Distillation.

Learnable Feedback Rescaling. As mentioned in Section 3.1, we rescale the feedback outputs, f_{feed} with some learnable scalar s_i for each block in the inner loop. This simple multiplication operation is cheap, and allows us to use a single feedback computation to improve the features used by all blocks within the inner loop. Furthermore, by zero-initializing and learning s we are able to avoid needing to set any hard-coded hyperparameters.

Fast Approximate Distillation Standard diffusion models train with a reconstruction loss. We use this same loss, and a novel pseudo-self-distillation loss between the output of diffusion with ILF (student) and diffusion without ILF (teacher). To align with our objective to predict future noise outputs, we perform the distillation using less noisy images. Specifically, whenever our ILF input during training is noised to step t , we noise the teacher input to step $t/2$. We then compute standard mean squared error loss between their predictions. Note that while we refer to diffusion with

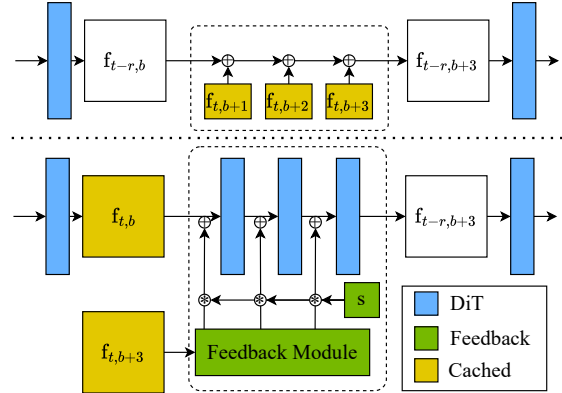


Figure 6. Caching (top) vs. ILF (bottom). We show how we use a partial diffusion forward pass to compute $f_{t,b+3}$, which we then use to compute $f_{t-r,b+3}$. We can use fewer of ILF’s heavy steps to ultimately achieve better quality-time trade-offs than caching’s cheap steps.

ILF as the student, only the feedback module and the rescaling parameters are learnable. This novel formulation saves on training cost.

3.3. Feedback-aware Inference Scheduling

With ILF, we are training the feedback to take inputs for one time step t , and produce predictions for a future time step $t-r$. However, in practice, we still need to denoise the actual original input, x_t . Treating this as if it were a more clean input, x_{t-r} , and removing the corresponding amount of noise, would be counterproductive. So, we still use the sigmas corresponding to t rather than $t-r$ for the backwards diffusion process itself. Thus, our method is akin to conditioning the model to generate a more reliable noise prediction, which can be used reliably for more spacing diffusion (fewer inference steps).

However, time step is not only used for the noise subtraction process. Rather, it is also a condition for the diffusion backbone itself. Hence, we must change the time condition used for all computation in the each forward pass that occurs *after* the feedback module forward. For the subsequent computation, we find that using an intermediate step, weighted for the size of the inner loop, is appropriate. So, for an inner loop with m blocks in a model comprised of n total blocks, and a scheduler with consecutive time steps t and $t-i$, we compute the intermediate post-feedback time step, t_{post} , with

$$t_{\text{post}} = t - i * (n/m) \quad (4)$$

We refer to this strategy in Section 4 as “Rescaling,” as opposed to “Uniform” computation of $t_{\text{post}} = t - i/2$. We

Table 1. Main results, high-quality text-to-image generation, speedups compared to 20 step DPM-Solver++ generations. We bold the best efficient results (the higher of each metric between ILF, caching, and the baseline at 12 steps). For some metrics ILF even outperforms the 20 step baseline.

Model	Settings		Latency		Prompt-aware Metrics		FID ↓	CLIP Image Quality Assessment			
	Res.	# Steps	# Blocks	s / img	Image Reward	CLIP	MJHQ	Good	Noisy ↓	Colorful	Natural
PixArt-alpha	1024	20	560	6.38	94.43	28.96	6.51	92.71	23.92	57.79	66.26
PixArt-alpha	1024	12	336	3.69 (1.7x)	90.41	28.94	6.86	92.75	25.38	56.07	64.71
PixArt-alpha w/ cache	1024	20	326	3.63 (1.8x)	82.49	28.86	6.85	91.20	29.47	50.38	63.38
PixArt-alpha w/ ours	1024	10	332	3.63 (1.8x)	91.71	28.98	6.13	90.60	24.91	59.18	66.97
PixArt-sigma	1024	20	560	6.63	83.87	29.28	7.28	90.32	27.98	59.60	69.12
PixArt-sigma	1024	12	336	3.81 (1.7x)	81.82	29.43	6.86	89.65	31.78	63.26	65.01
PixArt-sigma w/ cache	1024	20	326	3.75 (1.8x)	71.93	29.33	7.44	84.24	38.49	48.02	72.24
PixArt-sigma w/ ours	1024	10	332	3.75 (1.8x)	79.74	29.45	6.79	88.26	30.22	69.28	63.56
PixArt-alpha	512	20	560	1.06	92.03	29.06	7.13	92.79	17.17	66.17	51.59
PixArt-alpha	512	12	336	0.62 (1.7x)	88.42	29.02	7.86	94.49	18.95	71.57	48.06
PixArt-alpha w/ cache	512	20	326	0.59 (1.8x)	82.95	28.93	6.56	92.04	19.52	61.99	48.67
PixArt-alpha w/ ours	512	10	332	0.59 (1.8x)	89.47	29.11	7.20	92.67	16.89	69.31	50.18
PixArt-sigma	512	20	560	1.14	94.17	29.12	7.99	89.57	20.04	65.67	52.69
PixArt-sigma	512	12	336	0.66 (1.7x)	94.17	29.20	7.21	90.82	19.75	68.47	48.93
PixArt-sigma w/ cache	512	20	326	0.66 (1.7x)	87.08	29.09	7.05	87.73	22.32	59.38	53.26
PixArt-sigma w/ ours	512	10	332	0.66 (1.7x)	95.28	29.24	6.92	89.35	19.91	73.06	45.87

also observe that as we continue to train the feedback mechanism, it will “over-fit” – providing cluttered, over-saturated outputs. While on face this seems problematic, we actually find we can take advantage of it. First, we modify our rescaling to anneal over time. For $t = 999$, we use t_{post} as in Equation 4. However, for subsequent steps, we instead compute t_{post} as

$$t_{\text{post}} = t - \max(i * (n/m) * (t/1000), 10) \quad (5)$$

While we find this “Annealing” helps to improve results (see Figure 7), it is not fully optimal. By “Skipping” some feedback on some of the middle inference steps, we are able to perform inference even faster, while improving the quality from ILF. We provide some useful configurations and empirical exploration in Section 4.

4. Experiments

4.1. Experimental Setup

We use 5 pre-trained diffusion models, DiT, PixArt-alpha 512x512, PixArt-alpha 1024x1024, PixArt-sigma 512x512, and PixArt-sigma 1024x1024. All experiments and results are computed on NVIDIA H100 GPUs, unless otherwise specified, and scale up the quantity as necessary for each experiment. Whenever we train our feedback module for text-to-image, we use learning rate 10^{-6} , batch size 2048, and train for 5 epochs across a proprietary set of 2 million high-quality text-image pairs. For class-to-image, we use learning rate $5 * 10^{-6}$, batch size 8192, and train for 10 epochs on the approximately 1,281,167 ImageNet [40]

class-image pairs. Unless otherwise indicated, we use DPM-Solver++ [24]. For the base 28-block DiT with 749M frozen parameters, our feedback adds 26.7M learnable parameters. ILF adds 21.3M learnable parameters to 611M frozen parameters for both 28-block PixArt-alpha and 28-block PixArt-sigma.

To assess our performance, we rely on both examples and metrics. Unless otherwise specified, example images are drawn from sample prompts we provide in the supplementary material. For quantitative results, we compute Image Reward [49], using the prompts and procedure from the official code repository. We also compute MJHQ [20] FID with clean-fid [31], CLIP score [10] on the generations from complex prompts we provide in the supplementary, and CLIP IQA [47] on images generated from the Image Reward prompts. When computing CLIP IQA, we report the standard CLIP IQA Score as “Good” (since it is the result of competing “Good” and “Bad” text prompts), as well as its measurements of “Noisy,” “Colorful,” and “Natural.” In general we prioritize Image Reward due to its good correlation with human judgments, but other metrics offer further confirmation of our method’s utility.

4.2. Main Results

We show that our method works exceptionally well for fast, high quality text-to-image generation in Table 1. For settings for our method, we train feedback to create an inner loop from block $b = 8$ to block $b = 19$, and at inference we perform feedback only for the first two and last two steps. We outperform the caching baseline (where we cache the

middle 18 blocks, re-computing features once every 3 steps) for nearly every metric across both models at both resolutions. Furthermore, we even achieve comparable or better results in many metrics compared to the inefficient baseline.

In addition to seconds per image, we measure latency by number of block forwards to generate the image. To compute block forwards, we add up the total number of passes through a transformer block. Since the blocks are all the same size and shape (including our feedback block), this is a straightforward, reliable way to compare complexity across methods. Since all these models have 28 blocks, a standard forward pass is 28 block forwards. Our inner loop consists of 12 blocks, and the feedback itself is 1 block; hence, when performing our feedback with 10 step inference, skipping feedback for the middle 6 steps, yields $332 = (28*10) + (13*4)$ block forwards. We report latency both in terms of block forwards and seconds since exact time on various GPUs and with various optimizations may vary, but since our feedback block is identical to the backbone blocks, it can be considered as simply 1 extra block forward per step, and thus we can get a good approximation of latency before even running inference.

While we sample a variety of metrics for thoroughness, none correlate perfectly with human judgment of quality. Nevertheless, we provide some numerical ablations in Figure 7 and Figure 8. For qualitative results, for coverage of more diverse settings, we compare 1.4x speedups (we use 12 steps instead of 10, and skip feedback on the inner 8 steps) in Figure 9, and for 1.8x speedups in Figure 12 in the Appendix. While Table 1 and Figure 12 show that ILF performs well in the 1.8x speedup setting, in Figure 9 we show our results are clearly superior to caching even for less dramatic speedups, where our 1.5x has better visual quality than caching at 1.4x.

4.3. Ablations

We first show ILF works for class-to-image generation in Table 2. While the speedups are less dramatic, the ImageNet FID improvements are non-trivial. Since the method itself is designed primarily for text-to-image generation, we use this to showcase the flexibility of the method for a different task. We choose settings to safely give both some speedup and FID improvement, but with more tuning, or else aiming for equal FID, one could achieve better ImageNet FID with ILF.

We verify that our method is not overly sensitive to the location of the inner loop in Table 3. Indeed, as long as the loop is not at the end of the model, results are quite comparable among various settings. Note that for the smaller loops we only rescale the feedback, whereas for the larger loops we both rescale and skip feedback for the middle 8 steps.

We provide some understanding of the impact of train-

ing time on quality in Figure 7 and of the relationship between inference steps and image reward in Figure 8. Image quality increases over training time until it saturates around 5,000 iterations. However, not all inference strategies are equally well-suited. Similarly, quality increases with more inference steps. As Figure 8 suggests, our method has a substantial edge in quality across the range of intermediate to high steps (we neither consider nor report extremely low step results). As a disclaimer, Image Reward, while it correlates with human judgment better than most metrics, is still not perfect; from our observation, it is not overly sensitive to some of the lighting, sharpening, and over-detailing artifacts our method will introduce if its over-fitting is not properly mitigated.

We perform an ablation to determine which feedback steps to skip, with sample generations shown in Figure 10. We find that skipping feedback for the inner steps yields the most consistently good results, which lines up with our intuition that the first steps are the most important for determining good layouts, and the last steps are quite important for guaranteeing good fine details. So, it is best to perform our powerful diffusion feedback on those steps.

We also demonstrate that training with our results with Fast Approximate Distillation match results from training with the more expensive standard distillation (multiple teacher steps, in this case 8), in Figure 11. Since instead of 8 teacher steps, we only need 1, we are able to achieve good results with cheaper training. For further ablations, explorations, and examples, see the Appendix.

5. Conclusion

We propose diffusion with Inner Loop Feedback (ILF) for diffusion inference with fewer, more powerful steps. As a result, we can leverage pre-trained models to synthesize high-quality images in less time. With Learnable Feedback Rescaling and Fast Approximate Distillation, we train feedback for efficient megapixel image generation in approximately 100 GPU hours. Our method outperforms the training-free caching baseline, and is substantially cheaper and more flexible than any distillation-based alternative. Future work could explore using ILF to cheaply finetune a model on new data, as well as try to achieve better performance at extremely low steps. By accounting for encoder-decoder skip connections, ILF could even be adapted for U-Nets, though we consider this out of scope due to DiT’s rising popularity.

References

- [1] Fan Bao, Shen Nie, Kaiwen Xue, Yue Cao, Chongxuan Li, Hang Su, and Jun Zhu. All are worth words: A vit backbone for diffusion models, 2023. 3
- [2] Andreas Blattmann, Robin Rombach, Huan Ling,

Table 2. Class-to-Image results, ImageNet, DiT 256x256. ILF has better FID at better speed. While we choose settings here that consistently *outperform* the non-accelerated FID, one could instead prioritize speed with ILF to *match*, rather than beat, the baseline.

Model	# Steps	# Blocks	s / img	FID ↓
DiT	12	336	0.14	4.50
DiT w/ ours	10	304	0.13 (1.1x)	4.06 (-0.47)
DiT	25	700	0.29	3.96
DiT w/ ours	20	584	0.24 (1.2x)	3.59 (-0.37)
DiT	50	1400	0.57	3.56
DiT w/ ours	40	1144	0.47 (1.2x)	3.31 (-0.25)

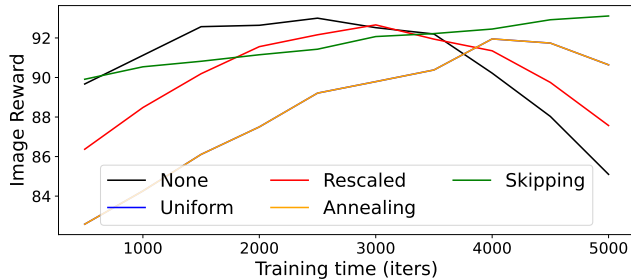


Figure 7. Training time effects on feedback scheduling, measured by Image Reward for PixArt-alpha 512x512.

Tim Dockhorn, Seung Wook Kim, Sanja Fidler, and Karsten Kreis. Align your latents: High-resolution video synthesis with latent diffusion models. In *Proceedings of the IEEE/CVF Conference on Computer Vision and Pattern Recognition (CVPR)*, pages 22563–22575, 2023. 3

- [3] Tim Brooks, Aleksander Holynski, and Alexei A. Efros. Instructpix2pix: Learning to follow image editing instructions. In *Proceedings of the IEEE/CVF Conference on Computer Vision and Pattern Recognition (CVPR)*, pages 18392–18402, 2023. 3
- [4] Junsong Chen, Jincheng Yu, Chongjian Ge, Lewei Yao, Enze Xie, Yue Wu, Zhongdao Wang, James Kwok, Ping Luo, Huchuan Lu, and Zhenguo Li. Pixart- α : Fast training of diffusion transformer for photorealistic text-to-image synthesis, 2023. 3
- [5] Junsong Chen, Chongjian Ge, Enze Xie, Yue Wu, Lewei Yao, Xiaoze Ren, Zhongdao Wang, Ping Luo, Huchuan Lu, and Zhenguo Li. Pixart- σ : Weak-to-strong training of diffusion transformer for 4k text-to-image generation, 2024. 3
- [6] Junsong Chen, Yue Wu, Simian Luo, Enze Xie, Sayak Paul, Ping Luo, Hang Zhao, and Zhenguo Li. Pixart- δ : Fast and controllable image generation with latent consistency models, 2024. 3
- [7] Prafulla Dhariwal and Alexander Nichol. Diffusion

Table 3. PixArt-alpha 512x512 loop size and location ablation, 12 steps. We compare a mix of small and large loops. We use our skipping inference scheduling for the larger loops to preserve the quality, which also gives better speedups.

Loop Size		Latency		Metrics	
Start	End	# Blocks	s / img	Image Reward	MJHQ FID ↓
0	5	420	0.78 (1.36x)	94.26	7.32
11	16	420	0.78 (1.36x)	93.80	7.07
22	27	420	0.78 (1.36x)	88.10	8.39
0	11	388	0.73 (1.44x)	93.10	6.47
8	19	388	0.73 (1.44x)	93.14	6.75
16	27	388	0.73 (1.44x)	90.20	7.56

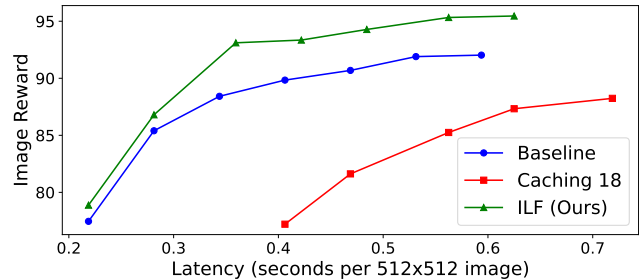


Figure 8. Image Reward vs. inference time, PixArt-alpha 512x512 for baseline, caching, and ILF. Ours is superior.

models beat gans on image synthesis. *Advances in neural information processing systems*, 34:8780–8794, 2021. 2, 3

- [8] Patrick Esser, Sumith Kulal, Andreas Blattmann, Rahim Entezari, Jonas Müller, Harry Saini, Yam Levi, Dominik Lorenz, Axel Sauer, Frederic Boesel, Dustin Podell, Tim Dockhorn, Zion English, Kyle Lacey, Alex Goodwin, Yannik Marek, and Robin Rombach. Scaling rectified flow transformers for high-resolution image synthesis, 2024. 3
- [9] Ian J. Goodfellow, Jean Pouget-Abadie, Mehdi Mirza, Bing Xu, David Warde-Farley, Sherjil Ozair, Aaron Courville, and Yoshua Bengio. Generative adversarial networks, 2014. 2
- [10] Jack Hessel, Ari Holtzman, Maxwell Forbes, Roman Le Bras, and Yejin Choi. Clipscore: A reference-free evaluation metric for image captioning, 2022. 6
- [11] Geoffrey Hinton, Oriol Vinyals, and Jeff Dean. Distilling the knowledge in a neural network, 2015. 4
- [12] Jonathan Ho, Ajay Jain, and Pieter Abbeel. Denoising diffusion probabilistic models. *Advances in Neural Information Processing Systems*, 33:6840–6851, 2020. 3
- [13] Jonathan Ho, William Chan, Chitwan Saharia, Jay Whang, Ruiqi Gao, Alexey Gritsenko, Diederik P. Kingma, Ben Poole, Mohammad Norouzi, David J.

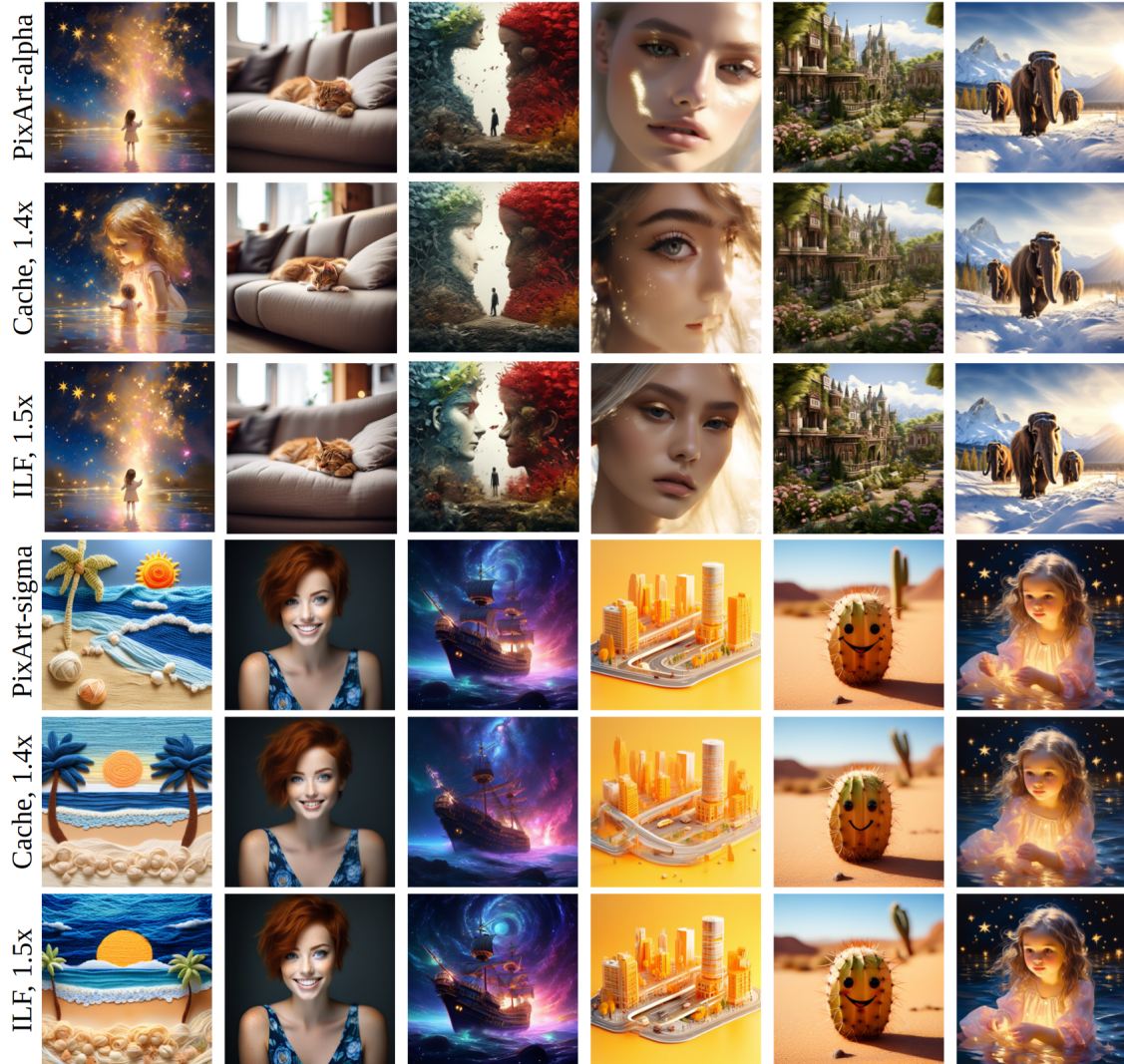


Figure 9. 512x512 results, alpha (top half) and sigma (bottom half), with baseline, caching, and our results, respectively. ILF yields images of similar content and quality to the un-accelerated baseline, and clearly superior to the caching, for both models. Zoom-in recommended.

Fleet, and Tim Salimans. Imagen video: High definition video generation with diffusion models, 2022. 3

[14] Zeyinzi Jiang, Chaojie Mao, Yulin Pan, Zhen Han, and Jingfeng Zhang. Scedit: Efficient and controllable image diffusion generation via skip connection editing, 2023. 4

[15] Tero Karras, Miika Aittala, Timo Aila, and Samuli Laine. Elucidating the design space of diffusion-based generative models, 2022. 3

[16] Bahjat Kawar, Shiran Zada, Oran Lang, Omer Tov, Huiwen Chang, Tali Dekel, Inbar Mosseri, and Michal Irani. Imagic: Text-based real image editing with diffusion models. In *Proceedings of the IEEE/CVF Conference on Computer Vision and Pattern Recognition (CVPR)*, pages 6007–6017, 2023. 3

[17] Diederik P Kingma and Max Welling. Auto-encoding variational bayes, 2014. 3

[18] Jonas Kohler, Albert Pumarola, Edgar Schönfeld, Artiom Sanakoyeu, Roshan Sumbaly, Peter Vajda, and Ali Thabet. Imagine flash: Accelerating emu diffusion models with backward distillation, 2024. 4

[19] Youngwan Lee, Kwanyong Park, Yoorhim Cho, Yong-Ju Lee, and Sung Ju Hwang. Koala: Empirical lessons toward memory-efficient and fast diffusion models for text-to-image synthesis, 2024. 4

[20] Daiqing Li, Aleks Kamko, Ehsan Akhgari, Ali Sabet, Linmiao Xu, and Suhail Doshi. Playground v2.5: Three insights towards enhancing aesthetic quality in text-to-image generation, 2024. 6

- [21] Senmao Li, Taihang Hu, Fahad Shahbaz Khan, Linxuan Li, Shiqi Yang, Yaxing Wang, Ming-Ming Cheng, and Jian Yang. Faster diffusion: Rethinking the role of unet encoder in diffusion models, 2023. 3
- [22] Haozhe Liu, Wentian Zhang, Jinheng Xie, Francesco Faccio, Mengmeng Xu, Tao Xiang, Mike Zheng Shou, Juan-Manuel Perez-Rua, and Jürgen Schmidhuber. Faster diffusion via temporal attention decomposition, 2024. 3
- [23] Yixin Liu, Kai Zhang, Yuan Li, Zhiling Yan, Chu-jie Gao, Ruoxi Chen, Zhengqing Yuan, Yue Huang, Hanchi Sun, Jianfeng Gao, Lifang He, and Lichao Sun. Sora: A review on background, technology, limitations, and opportunities of large vision models, 2024. 3
- [24] Cheng Lu, Yuhao Zhou, Fan Bao, Jianfei Chen, Chongxuan Li, and Jun Zhu. Dpm-solver++: Fast solver for guided sampling of diffusion probabilistic models, 2023. 3, 6
- [25] Simian Luo, Yiqin Tan, Longbo Huang, Jian Li, and Hang Zhao. Latent consistency models: Synthesizing high-resolution images with few-step inference, 2023. 4
- [26] Xinyin Ma, Gongfan Fang, and Xinchao Wang. Deep-cache: Accelerating diffusion models for free, 2023. 2, 3
- [27] Xinyin Ma, Gongfan Fang, Michael Bi Mi, and Xinchao Wang. Learning-to-cache: Accelerating diffusion transformer via layer caching, 2024. 3
- [28] Chenlin Meng, Robin Rombach, Ruiqi Gao, Diederik P. Kingma, Stefano Ermon, Jonathan Ho, and Tim Salimans. On distillation of guided diffusion models, 2023. 4
- [29] Alex Nichol, Prafulla Dhariwal, Aditya Ramesh, Pranav Shyam, Pamela Mishkin, Bob McGrew, Ilya Sutskever, and Mark Chen. Glide: Towards photorealistic image generation and editing with text-guided diffusion models, 2022. 3
- [30] Alexander Quinn Nichol and Prafulla Dhariwal. Improved denoising diffusion probabilistic models. In *International Conference on Machine Learning*, pages 8162–8171. PMLR, 2021. 3
- [31] Gaurav Parmar, Richard Zhang, and Jun-Yan Zhu. On aliased resizing and surprising subtleties in gan evaluation. In *CVPR*, 2022. 6
- [32] William Peebles and Saining Xie. Scalable diffusion models with transformers, 2023. 3
- [33] Dustin Podell, Zion English, Kyle Lacey, Andreas Blattmann, Tim Dockhorn, Jonas Müller, Joe Penna, and Robin Rombach. Sdxl: Improving latent diffusion models for high-resolution image synthesis, 2023. 3
- [34] Alec Radford, Jong Wook Kim, Chris Hallacy, Aditya Ramesh, Gabriel Goh, Sandhini Agarwal, Girish Sastri, Amanda Askell, Pamela Mishkin, Jack Clark, Gretchen Krueger, and Ilya Sutskever. Learning transferable visual models from natural language supervision, 2021. 3
- [35] Colin Raffel, Noam Shazeer, Adam Roberts, Katherine Lee, Sharan Narang, Michael Matena, Yanqi Zhou, Wei Li, and Peter J. Liu. Exploring the limits of transfer learning with a unified text-to-text transformer, 2023. 3
- [36] Aditya Ramesh, Prafulla Dhariwal, Alex Nichol, Casey Chu, and Mark Chen. Hierarchical text-conditional image generation with clip latents, 2022. 3
- [37] Robin Rombach, Andreas Blattmann, Dominik Lorenz, Patrick Esser, and Björn Ommer. High-resolution image synthesis with latent diffusion models, 2022. 3
- [38] Olaf Ronneberger, Philipp Fischer, and Thomas Brox. U-net: Convolutional networks for biomedical image segmentation, 2015. 3
- [39] Nataniel Ruiz, Yuanzhen Li, Varun Jampani, Yael Pritch, Michael Rubinstein, and Kfir Aberman. Dreambooth: Fine tuning text-to-image diffusion models for subject-driven generation. In *Proceedings of the IEEE/CVF Conference on Computer Vision and Pattern Recognition (CVPR)*, pages 22500–22510, 2023. 3
- [40] Olga Russakovsky, Jia Deng, Hao Su, Jonathan Krause, Sanjeev Satheesh, Sean Ma, Zhiheng Huang, Andrej Karpathy, Aditya Khosla, Michael Bernstein, Alexander C. Berg, and Li Fei-Fei. Imagenet large scale visual recognition challenge, 2015. 6
- [41] Amirmojtaba Sabour, Sanja Fidler, and Karsten Kreis. Align your steps: Optimizing sampling schedules in diffusion models, 2024. 3
- [42] Chitwan Saharia, William Chan, Saurabh Saxena, Lala Li, Jay Whang, Emily L Denton, Kamyar Ghasemipour, Raphael Gontijo Lopes, Burcu Karagol Ayan, Tim Salimans, Jonathan Ho, David J Fleet, and Mohammad Norouzi. Photorealistic text-to-image diffusion models with deep language understanding. In *Advances in Neural Information Processing Systems*, pages 36479–36494. Curran Associates, Inc., 2022. 3
- [43] Tim Salimans and Jonathan Ho. Progressive distillation for fast sampling of diffusion models, 2022. 4
- [44] Axel Sauer, Dominik Lorenz, Andreas Blattmann, and Robin Rombach. Adversarial diffusion distillation, 2023. 4
- [45] Pratheba Selvaraju, Tianyu Ding, Tianyi Chen, Ilya Zharkov, and Luming Liang. Fora: Fast-forward caching in diffusion transformer acceleration, 2024. 3

- [46] Jiaming Song, Chenlin Meng, and Stefano Ermon. Denoising diffusion implicit models, 2022. [3](#)
- [47] Jianyi Wang, Kelvin CK Chan, and Chen Change Loy. Exploring clip for assessing the look and feel of images. In *AAAI*, 2023. [6](#)
- [48] Felix Wimbauer, Bichen Wu, Edgar Schoenfeld, Xiaoliang Dai, Ji Hou, Zijian He, Artsiom Sanakoyeu, Peizhao Zhang, Sam Tsai, Jonas Kohler, Christian Rupprecht, Daniel Cremers, Peter Vajda, and Jialiang Wang. Cache me if you can: Accelerating diffusion models through block caching, 2024. [2](#), [3](#)
- [49] Jiazheng Xu, Xiao Liu, Yuchen Wu, Yuxuan Tong, Qinkai Li, Ming Ding, Jie Tang, and Yuxiao Dong. Imagereward: Learning and evaluating human preferences for text-to-image generation, 2023. [6](#)
- [50] Yanwu Xu, Yang Zhao, Zhisheng Xiao, and Tingbo Hou. Ufogen: You forward once large scale text-to-image generation via diffusion gans, 2023. [4](#)
- [51] Ling Yang, Zhilong Zhang, Yang Song, Shenda Hong, Runsheng Xu, Yue Zhao, Wentao Zhang, Bin Cui, and Ming-Hsuan Yang. Diffusion models: A comprehensive survey of methods and applications, 2024. [2](#)
- [52] Tianwei Yin, Michaël Gharbi, Richard Zhang, Eli Shechtman, Fredo Durand, William T. Freeman, and Taesung Park. One-step diffusion with distribution matching distillation, 2023. [4](#)
- [53] Hui Zhang, Zuxuan Wu, Zhen Xing, Jie Shao, and Yugang Jiang. Adadiff: Adaptive step selection for fast diffusion, 2023. [4](#)

Accelerate High-Quality Diffusion Models with Inner Loop Feedback

Supplementary Material

We provide some more qualitative results, these from MJHQ prompts, in Figure 12. We also provide Figure 13 and Figure 14 as complements to Figure 9, where these have crops that we zoom in on to help the reader observe fine-grained differences. We provide a complement to Table 1, with results for 1.4x-1.5x speedups in Table 4. Whenever we cache with 1.4x-1.4x, we skip the inner 18 blocks every other step (rather than twice per 3 steps). For our feedback inference scheduling, we skip feedback on the inner 8 steps on a 12 step schedule for 1.4x-1.5x, and the inner 6 steps on a 10 step schedule for 1.7x-1.8x. We would like to emphasize ILF’s outstanding Image Reward and visual appearance, even compared to the non-accelerated baselines, in addition to the fact that for the 28 points of comparison in Table 1, it is superior for 19, and the second best for 6. In Table 5, we show all metrics for the experiments introduced in Table 3.

We show the effect of skipping the feedback for different amounts of steps in Figure 15. Without skipping enough steps, images can be distorted. We observe overall highest quality, without distortions, when skipping the middle 8 steps for a 12 step inference schedule.

In Figure 16 we perform an exploration where we compare our inference strategies on small and large loops. We find that for smaller loops, simply rescaling tends to be the best. However, for larger loops, we need to skip feedback on some steps to avoid distortions. While initially this would seem problematic, this is actually a blessing in disguise. We can save time by skipping feedback on some steps, and the feedback is powerful enough to give good quality by using it on the initial and final steps.

To determine our caching configuration, we run a brief search over some simple options. We use ‘inner’ for our main experiments since it gives superior results according to both quantitative and qualitative inspection. We show qualitative results for different caching schemes in Figure 17, and quantitative results in Table 6. We try caching, for every other step, the first c blocks, the last c blocks, the outer c blocks, the inner c blocks, and evenly-spaced c blocks (alternating). We show results for $c = 14$, PixArt-alpha 512x512. We find that caching first blocks results in blurriness. Caching last blocks results in detrimental distortions and artifacts. Caching outer blocks is better, but still somewhat blurry. While ‘last’ has similar Image Reward to ‘inner’ we prefer ‘inner’ since it doesn’t result in odd or unnatural generations, that may not be punished appropriately by the Image Reward. Caching is merely a baseline, and not the focus of our paper. Nevertheless this limited investigation of caching for DiTs for text-to-image generation should

hopefully help the community with training-free efficiency approaches.



Figure 10. Visual examples of different skipping feedback for different time steps at inference time, skipping feedback for the alternating steps (top), first steps only (second), last steps only (third), outer steps (fourth) and then inner steps (bottom). Skipping feedback for inner steps is best, with good overall structure and high quality details, without distortions.



Figure 11. We show results for training with no distillation (top), with standard teacher distillation (middle), and then with our fast approximate teacher distillation (bottom). Ours gives the same good results as standard ablation, but with lower training cost.

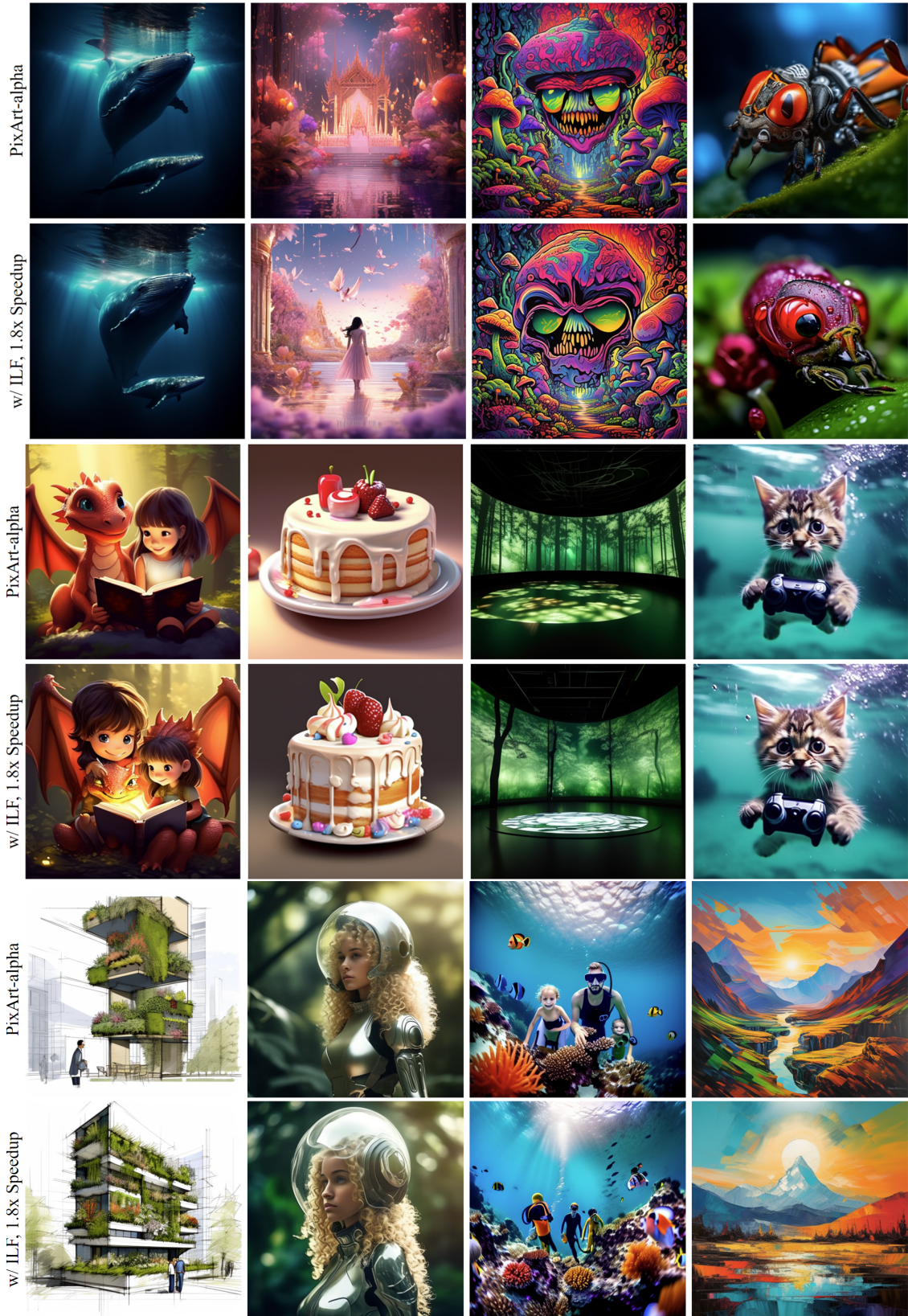


Figure 12. Bonus results page, large size for print readers. Alternating rows of baseline vs. ours, PixArt-alpha 512x512, with **1.8x speedup**. See supplementary for further examples. The top two rows should where our results are roughly equal, second row shows some failure cases, and third row shows some instances where ours are superior.

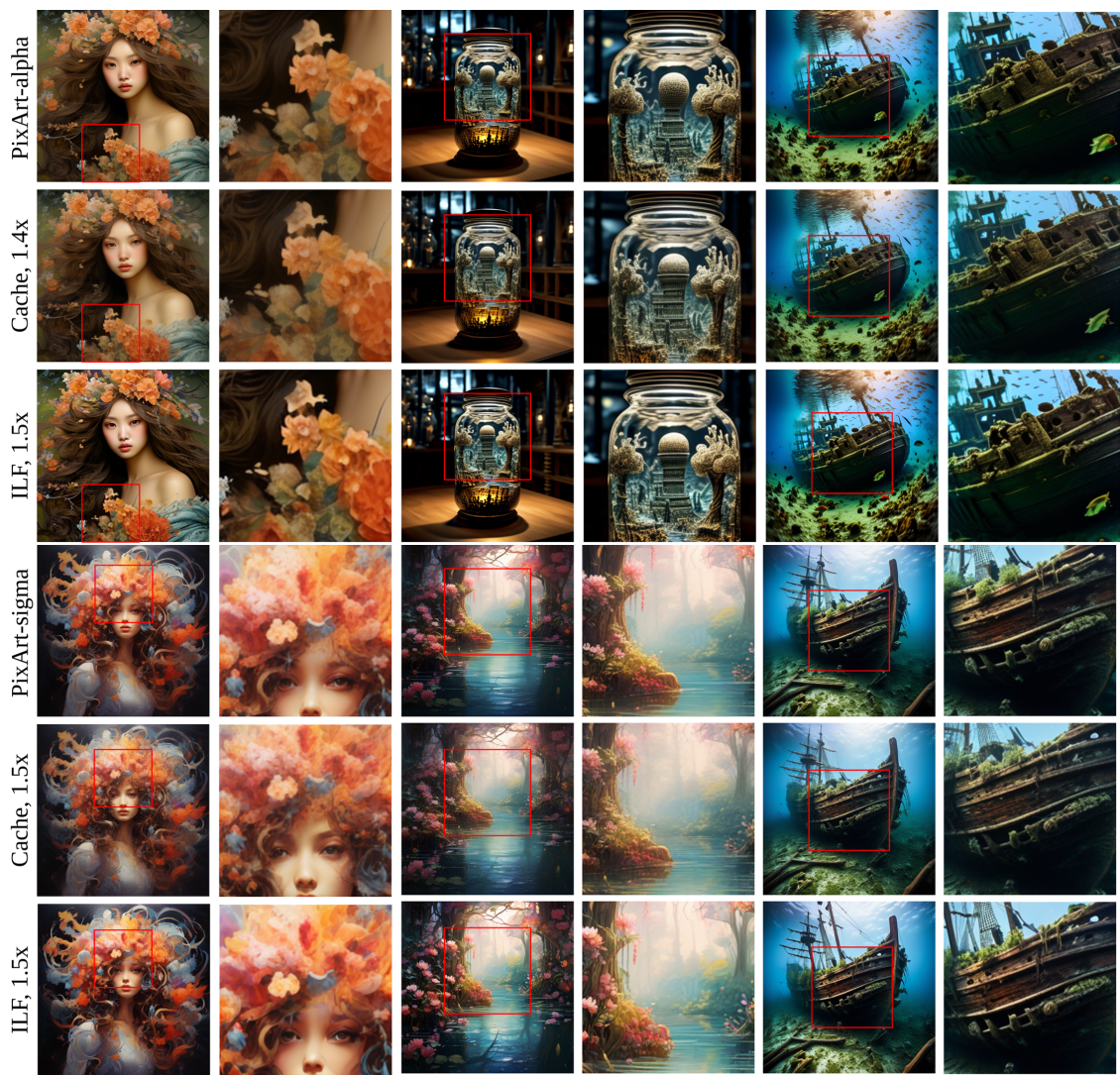


Figure 13. 512x512 results, alpha (top 3 rows) and sigma (bottom 3 rows), with baseline, caching, and our results, respectively, for 1.4x-1.5x acceleration. ILF yields images of similar content and quality to the un-accelerated baseline, and clearly superior to the caching, for both models. Zoomed in and cropped for convenience.

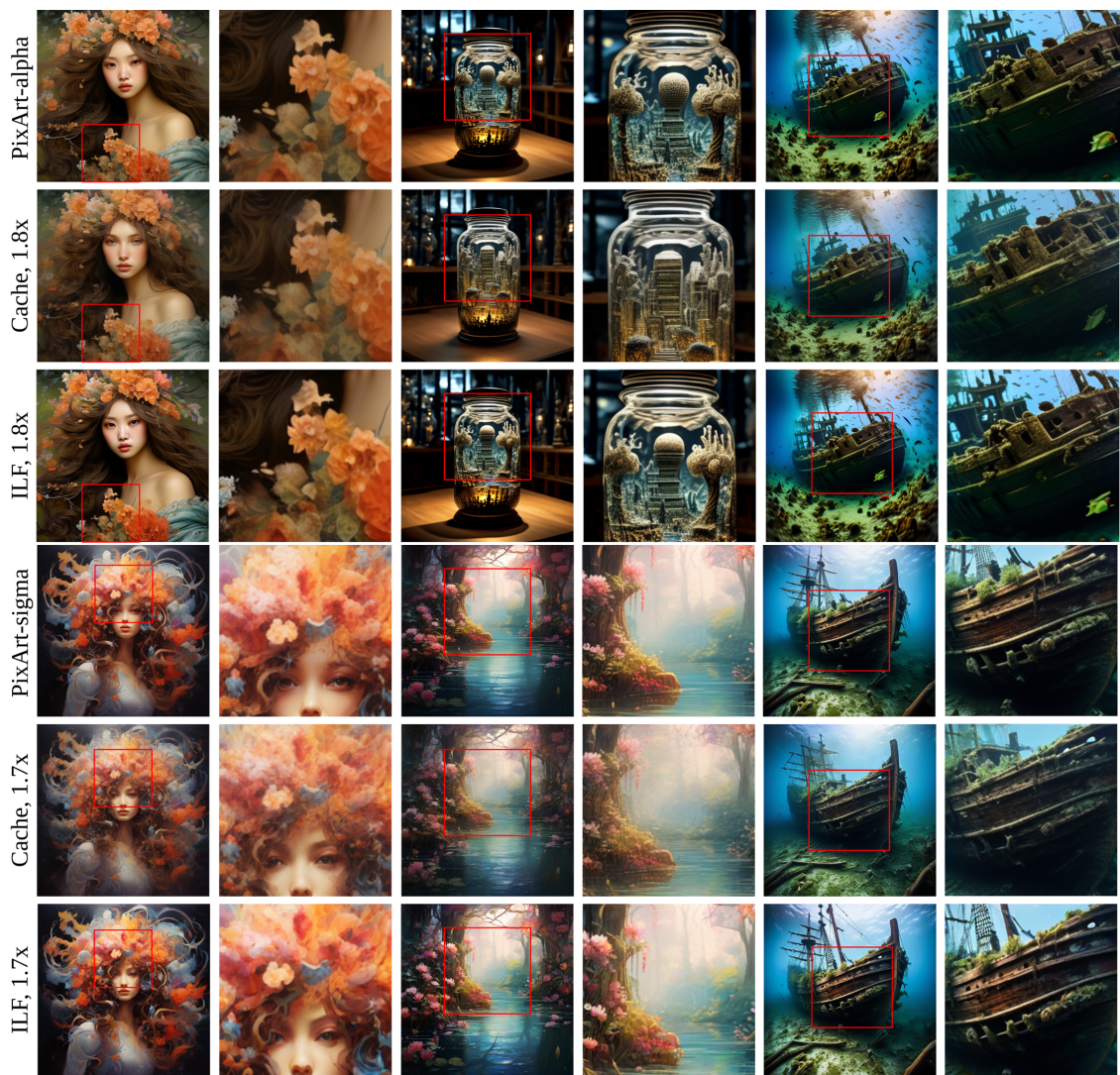


Figure 14. 512x512 results, alpha (top 3 rows) and sigma (bottom 3 rows), with baseline, caching, and our results, respectively, for 1.7x-1.8x acceleration. ILF yields images of similar content and quality to the un-accelerated baseline, and clearly superior to the caching, for both models. Zoomed in and cropped for convenience.

Table 4. Extension of main results for less aggressive, 1.4x speedups compared to 20 step DPM-Solver++ generations. We bold the best *overall* results, and underline the second best.

Model	Settings		Latency		Prompt-aware Metrics		FID ↓	CLIP Image Quality Assessment			
	Res.	# Steps	# Blocks	s / img	Image Reward	CLIP	MJHQ	Good	Noisy ↓	Colorful	Natural
PixArt-alpha	1024	20	560	6.38	<u>94.43</u>	<u>28.96</u>	6.51	92.71	<u>23.92</u>	<u>57.79</u>	<u>66.26</u>
PixArt-alpha w/ cache	1024	20	380	4.25 (1.5x)	91.41	28.95	<u>6.09</u>	<u>92.61</u>	26.07	54.11	65.14
PixArt-alpha w/ ours	1024	12	388	4.25 (1.5x)	96.68	29.03	5.92	90.88	23.84	61.39	67.46
PixArt-sigma	1024	20	560	6.63	<u>83.87</u>	29.28	7.28	90.32	<u>27.98</u>	<u>59.60</u>	<u>69.12</u>
PixArt-sigma w/ cache	1024	20	380	4.38 (1.5x)	79.63	<u>29.35</u>	6.56	87.09	33.70	52.31	72.48
PixArt-sigma w/ ours	1024	12	388	4.50 (1.4x)	84.06	29.41	<u>6.95</u>	<u>89.06</u>	26.42	67.94	67.92
PixArt-alpha	512	20	560	1.06	<u>92.03</u>	<u>29.06</u>	7.13	92.79	<u>17.17</u>	<u>66.17</u>	<u>51.59</u>
PixArt-alpha w/ cache	512	20	380	0.72 (1.5x)	88.24	29.03	6.52	92.72	18.20	63.52	50.01
PixArt-alpha w/ ours	512	12	388	0.73 (1.5x)	93.17	29.11	<u>6.78</u>	<u>92.74</u>	16.11	<u>69.80</u>	52.14
PixArt-sigma	512	20	560	1.14	<u>94.17</u>	29.12	7.99	89.57	<u>20.04</u>	<u>65.67</u>	<u>52.69</u>
PixArt-sigma w/ cache	512	20	380	0.75 (1.5x)	92.38	<u>29.15</u>	6.78	88.68	20.82	62.19	53.53
PixArt-sigma w/ ours	512	12	388	0.77 (1.5x)	96.31	29.19	<u>7.31</u>	<u>89.10</u>	19.13	70.96	50.55

Table 5. Main results, high-quality text-to-image generation.

Loop Size		Latency		Prompt-aware Metrics		FID ↓	CLIP Image Quality Assessment			
Start	End	# Blocks	s / img	Image Reward	CLIP	MJHQ	Good	Noisy ↓	Colorful	Natural
0	5	420	0.78 (1.36x)	94.26	29.17	7.32	92.01	17.32	75.54	52.81
11	16	420	0.78 (1.36x)	93.80	29.15	7.07	92.86	15.88	73.63	53.50
22	27	420	0.78 (1.36x)	88.10	29.03	8.39	92.61	18.05	65.37	49.77
0	11	388	0.73 (1.44x)	93.10	29.15	6.47	92.99	15.72	70.56	53.16
8	19	388	0.73 (1.44x)	93.14	29.11	6.75	92.74	16.11	69.79	52.13
16	27	388	0.73 (1.44x)	90.20	29.05	7.56	92.52	17.73	65.68	50.08

Table 6. Caching exploration, different locations for PixArt-alpha, 512x512 images. Same settings as Figure 17.

Caching Location	# Steps	# Block Forward	Image Reward
First	20	440	83.35
Last	20	440	89.54
Outer	20	440	87.75
Inner	20	440	<u>89.37</u>
Alternating	20	440	83.98



Figure 15. We try skipping feedback more and less often for 12 step inference. On the top, we do not skip any feedback (equivalent to our feedback time step rescaling strategy). On the next row, we skip the middle 4 steps, then on the next row the middle 8 steps, and finally, for the bottom row, we skip the inner 10 steps. All results use PixArt-alpha, 512x512 images, inner loop from block $b = 8$ to $b = 19$. We trade off quantity of details (such as number of stars) and sharpness in exchange for smoother, better lit, more natural images. Notably this is controllable, and can be adjusted according to the practitioner’s preference.



Figure 16. We compare different inference strategies (default, rescaled, and skipping, in order) for two different loop sizes; on the top, a larger loop from block $b = 8$ to $b = 19$, and on the bottom, a smaller loop connecting $b = 0$ to $b = 5$. Note that when using default inference, without accounting for the feedback, the image content and quality degrades (zoom-in required). For both models this default inference results in images with excessive details and overly bright, over-saturation. Using our feedback time step rescaling (2nd and 5th rows) helps mitigate this to an extent, and for the smaller loop, this produces the best images. However, for the larger loop, we get the most natural, but still detailed images, when both rescaling and skipping feedback on some time steps (bottom row). One can control the level of detail by changing the frequency of the skipping.

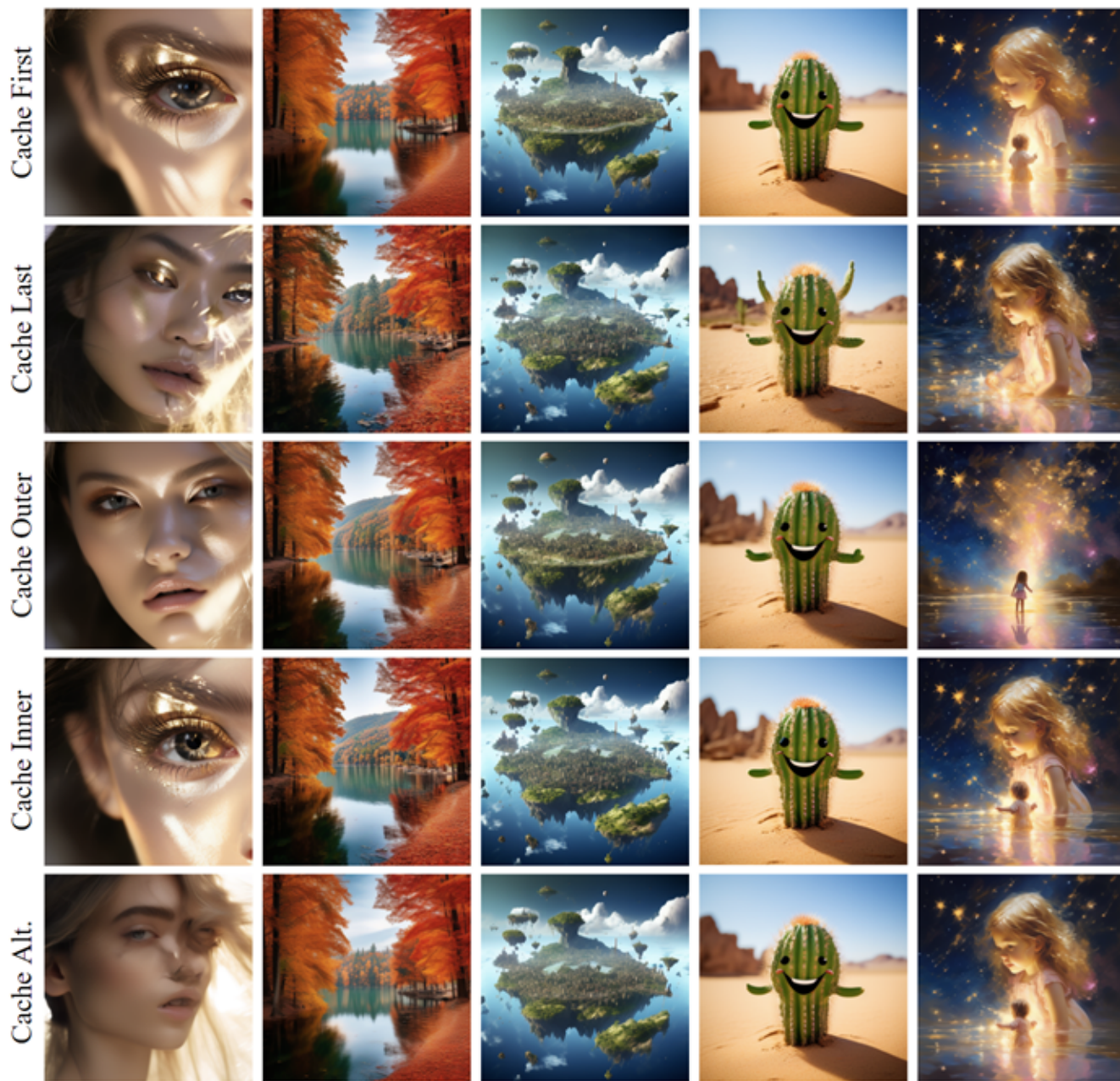


Figure 17. We compare different caching locations for PixArt-alpha, 512x512 images, caching 14 blocks every other step. We cache the first blocks (top), last blocks, outer blocks, inner blocks, and alternating blocks (bottom). Notice the blurriness when caching first and alternating (Alt.) blocks, the distortions when caching last blocks, and overall poor quality when caching outer blocks. None of these are ideal, but we find the best performance for inner; thus, in our main results we compare to caching inner blocks.